Surface Chemistry of Boron Oxidation. 1. Reactions of Oxygen and Water with Boron Films Grown on Ta(110)

Yajun Wang, Jingfu Fan, and Michael Trenary*

Department of Chemistry, M/C 111, University of Illinois at Chicago, Chicago, Illinois 60680

Received August 26, 1992. Revised Manuscript Received November 23, 1992

The reactions of O_2 and D_2O with thin boron films grown on Ta(110) through the decomposition of B_2H_6 at 650–700 K were studied with X-ray photoelectron spectroscopy (XPS) and temperature-programmed desorption (TPD). The surface oxygen coverage, as measured by the area of the O(1s) peak at a binding energy of 532–534 eV, was monitored as a function of O_2 and D_2O exposure and surface temperature. The oxygen uptake is low at room temperature but increases with increasing temperature and reaches a maximum at 1000–1100 K for O_2 exposures and at a temperature greater than 800 K for D_2O exposures. TPD measurements show that the surface oxide desorbs as B_2O_2 at 1100–1250 K. XPS shows that the surface oxide gives rise to a B(1s) peak at a binding energy of 193.5 eV. This is compared to XPS results for B_2O_3 and B_2O_2 directly deposited on the boron film which have B(1s) binding energies of 193.5 and 192.6 eV, respectively. This comparison clearly shows that the reaction with O_2 or D_2O produces surface B_2O_3. As the surface temperature is increased, this B_2O_3 reacts with substrate boron to produce B_2O_2(g).

Introduction

The surface chemistry associated with the oxidation of elemental boron is of interest for several reasons. The reaction $4B(s) + 3O_2(g) \rightarrow 2B_2O_3$ is highly exothermic with a ΔH of −1272 kJ mol^{-1}. This has led to numerous combustion studies oriented toward the use of boron as a rocket fuel.[1-8] In addition, boron and boron compounds are often added to carbon–carbon composites to inhibit carbon oxidation at high temperatures.[9-13] It is assumed that the boron is oxidized to B_2O_3 which is then thought to either seal cracks or block active sites on the carbon surface.[13] The high melting point of boron of 2360 K means that oxidation of boron necessarily takes place at the gas/solid interface. This in turn suggests that the methods of modern surface science can be profitably employed to gain a more detailed understanding of the surface processes involved in the reaction of O_2 with boron to make B_2O_3.

The present paper complements our earlier study of the reaction of O_2 with the (111) surface of a single crystal of β-rhombohedral boron.[14] There are three principal reasons for conducting these additional experiments on the B/Ta(110) surface. First, a comparison of results obtained on the amorphous boron film with the results on the well-ordered single-crystal surface can provide information on the role of surface morphology in the reactivity. Combustion studies of boron particles indicate that amorphous boron is more reactive than crystalline boron.[5] The second reason concerns the practical experimental advantages of the B/Ta(110) system. As reported in our earlier paper,[14] it is difficult to prepare, mount, and accurately measure the temperature of boron single crystals for UHV surface science studies. The crystals also have the unfortunate tendency to shatter into small pieces after thermal cycling. In contrast, the use of boron films on Ta(110) offers all of the usual practical advantages of working with metal single crystals; spot-welding can be used to attach heating/support wires and thermocouples to the crystal edges; the high thermal conductivity of metals combined with the good thermal contact between the crystal and a spot-welded thermocouple makes temperature measurements more reliable. Third, large single crystals of boron are no longer available commercially and are difficult to grow.[15] For this reason development of the field of boron surface science would be severely limited if alternatives to boron single-crystal samples were not available.

We have conducted a few experiments using D_2O in addition to the O_2 experiments. The results obtained with D_2O are described only briefly because they are virtually identical to the results obtained with O_2. This paper is followed by a study of the reaction of boron films grown on Ta(110) with both B_2O_3 and B_2O_2 directly deposited on the surface.[16] The latter paper complements an earlier study of the reaction of B_2O_3 with the (111) surface of β-rhombohedral boron.[17]

* To whom correspondence should be addressed.

(1) King, M. L. *J. Spacecraft* **1982**, *19*, 294.
(2) Talley, C. P. *Aero/Space Eng.* **1959**, *18*, 37.
(3) Macek, A.; Semple, J. M. *Comb. Sci. Technol.* **1969**, *1*, 181.
(4) Macek, A.; Semple, J. M. Proceedings of the 13th Symposium (Int.) on Combustion; The Combustion Institute: Pittsburgh, PA, 1970; pp 859–868.
(5) Mohan, G.; Williams, F. A. *AIAA J.* **1972**, *10*, 776.
(6) Li, S. C.; Williams, F. A.; Takahshi, F. Proc. 22nd Symp. (Int.) on Combustion; The Combustion Institute: Pittsburgh, PA, 1988; pp 1951–1960.
(7) Glassman, I.; Williams, F. A.; Antaki, P. Proc. 20th Symp. (Int.) on Combustion; The Combustion Institute: Pittsburgh, PA, 1984; pp 2057–2064.
(8) Yetter, R. A.; Cho, S. Y.; Rabitz, H.; Dryer, F. L.; Brown, R. C.; Kolb, C. E. Proc. 22nd Symp. (Int.) on Combustion; The Combustion Institute: Pittsburgh, PA, 1988; pp 919–929.
(9) Jones, L. E.; Thrower, P. A. *Carbon* **1991**, *29*, 251.
(10) Sheehan, J. E. *Carbon* **1989**, *27*, 709.
(11) McKee, D. W. *Carbon* **1987**, *25*, 551.
(12) Ehrburger, P.; Baranne, P.; Lahaye, J. *Carbon* **1986**, *24*, 495.
(13) McKee, D. W.; Spiro, C. L.; Lamby, E. J. *Carbon* **1984**, *22*, 507.
(14) Foo, W. C.; Ozcomert, J. S.; Trenary, M. *Surf. Sci.* **1991**, *255*, 245.
(15) Borchert, W.; Dietz, W.; Kölker, H. *Z. Angew. Phys.* **1970**, *29*, 277.
(16) Wang, Y.; Trenary, M. *Chem. Mater.*, following article in this issue.
(17) Foo, W. C.; Ozcomert, J. S.; Trenary, M. *Surf. Sci.* **1992**, *262*, 88.

0897-4756/93/2805-0192$04.00/0

Experimental Section

The apparatus used in these studies has been described in detail elsewhere.[14,17,18] Briefly, the experiments were conducted in an ultrahigh-vacuum (UHV) chamber (base pressure $\leq 1 \times 10^{-10}$ Torr) equipped with low-energy electron diffraction (LEED) optics, an X-ray photoelectron spectroscopy (XPS) system, and a quadrupole mass spectrometer for residual gas analysis and temperature-programmed desorption (TPD) experiments.

The XPS system consists of a hemispherical electron energy analyzer (CLAM 100, VG Microtech) and a dual Mg/Al anode X-ray source (VG Microtech). The XPS binding energies were calibrated with a piece of silver foil, cleaned with Ar^+ ion sputtering, mounted above the sample. Using Mg Kα radiation and a constant analyzer pass energy of 20 eV which yields a nominal resolution of 1.0 eV, the silver foil gave a binding energy of 368.35 eV and a line width (fwhm) of 0.988 eV for the Ag($3d_{5/2}$) transition. This binding energy is within 0.1 eV of the calibration value of 368.29 ± 0.01 eV published by Anthony.[19] Except where otherwise noted, all XPS spectra were obtained using the Al anode (Al Kα radiation, 1486.6 eV) at a power of 600 W (15 kV, 40 mA emission current) with a constant analyzer pass energy of 50 eV corresponding to a nominal resolution of 1.8 eV.

A cylindrical rod of single crystal Ta with a quoted purity of 99.99% was purchased from Metal Crystals and Oxides, Ltd., of Cambridge, England. A disk 2 mm thick and 6 mm in diameter was cut from the rod to expose a surface within 0.5° of the (110) plane as determined by X-ray diffraction using the Laue back-reflection method. The oriented crystal was polished using succeedingly finer diamond polishing compounds down to a diamond particle size of 0.25 μm to a good mirror finish. The crystal was cleaned with acetone in an ultrasonic bath prior to mounting in the vacuum chamber. The Ta crystal was spot-welded to two 0.5-mm Ta wires which were attached to a copper block at the end of a manipulator rod. The sample was resistively heated by passing current through these Ta wires for TPD experiments. A partially shielded Ta filament was mounted directly behind the crystal for electron bombardment heating during initial sample cleaning and high temperature annealing. A 26% Re–W/5% Re–W (type C) thermocouple was spot-welded to the top edge and near the front surface of the crystal. The crystal could be heated to 1500–1600 K with resistive heating and to the melting point of 3270 K with electron bombardment heating. A heating rate of 1.9 K s^{-1} with resistive heating was used in the TPD experiments. The temperatures obtained with the thermocouple were compared with an optical pyrometer. There was usually about a 20 K difference between thermocouple and pyrometer readings. The temperatures reported here are all thermocouple readings unless otherwise noted.

Initial cleaning of the Ta crystal in the vacuum chamber was achieved by repeated cycles of Ar^+ sputtering (2-keV beam energy, 8–10-μA ion current at the sample, background Ar pressure of 5×10^{-5} Torr), annealing to 2700 K (pyrometer reading corrected for Ta emissivity and window transmission) in a background pressure (due to outgassing) of $\leq 1 \times 10^{-8}$ Torr. Cleaning was monitored with XPS and LEED. Figure 1a shows the full XPS spectrum from 0 to 1200 eV of the Ta(110) surface after a chamber bakeout but before the sample had been cleaned while Figure 1b is of the clean Ta surface. The spectra were taken at a constant analyzer pass energy of 50 eV (resolution of ≈1.8 eV) with Mg Kα radiation (1253.6 eV). The X-ray source was operated at a power of 300 W (15-kV bias, 20-mA emission current). The principal contaminants on the Ta surface were carbon and oxygen as indicated by the C(1s) peak at 284 eV and the O(1s) peak at 532 eV in Figure 1a. The carbon was easily removed during the first sputtering and annealing cycle, but considerably more effort was required to reduce the oxygen impurity level to less than 2%, based on relative O and Ta XPS sensitivities.[19,20] The insets

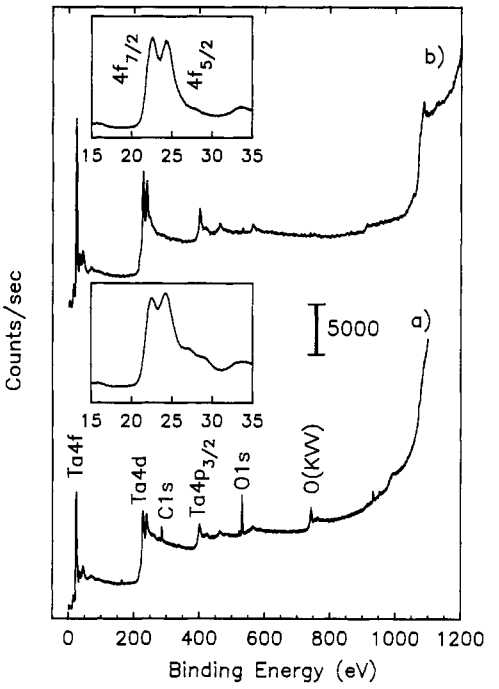

Figure 1. Full XPS spectrum of the Ta(110) surface (a) before and (b) after being cleaned.

to Figure 1a,b show the Ta(4f) region. For the clean surface, the Ta($4f_{7/2}$) peak is higher than the Ta($4f_{5/2}$) peak while the ratio is reversed for the contaminated surface. Because of the higher degeneracy of the $4f_{7/2}$ level, it should always have a greater intensity than the $4f_{5/2}$ peak, but since the O(2s) level is close to the Ta($4f_{5/2}$) level, the presence of a small amount of oxygen reverses the expected intensity. We have found this aspect of the Ta(4f) region to be a very sensitive diagnostic of an oxygen-free surface. Once clean, a sharp LEED pattern of the unreconstructed (110) surface was obtained.

The boron thin films were grown through the thermal decomposition of diborane, B_2H_6(g). The semiconductor purity B_2H_6(g) was obtained from Matheson Gas Products as a 1% mixture in 99.999% pure Ar. Diborane has been used by others for depositing boron on Mo(100)[21] and Ru(0001).[22–24] In the CVD growth of boron on Ta substrates, others have noted that the boron appears to first react with the Ta substrate to produce a layer of TaB_2.[25–27] Unlike boron films, which sublime after heating to high temperature, TaB_2 remains stable after heating to temperatures as high as 2700 K, consistent with the melting point of TaB_2 of ≈3500 K. Figure 2 shows an XPS spectrum of an oxygen-free TaB_2 layer. The B(1s) peak occurs at 189.0 eV for the TaB_2 layer and the Ta(4f)/B(1s) peak area ratio of 10.1 ● 1.3 yields $TaB_{1.94\pm0.15}$ as the stoichiometry of the boride layer, based on the relative B and Ta XPS sensitivities.[20] Our observation that the B(1s) binding energy of TaB_2 is 1.0 eV higher than in amorphous boron is consistent with results for other metal diborides.[20]

The boron thin films were grown on the TaB_2 layer with the sample temperature held in the range 650–700 K. The B_2H_6/Ar

(18) Foo, W. C. Ph.D. Dissertation, The University of Illinois at Chicago, 1991.
(19) Anthony, M. T. In *Practical Surface Analysis by Auger and X-ray Photoelectron Spectroscopy*; Briggs, D., Seah, M. P., Eds.; Wiley: New York, 1983.
(20) *Handbook of X-ray Photoelectron Spectroscopy*; Muilenburg, G. E., Ed.; Perkin-Elmer: Eden Praire, MN, 1979.
(21) Fryberger, T. B.; Grant, J. L.; Stair, P. C. *J. Vac. Sci. Technol. A* **1987**, *5*, 858.
(22) Rodriguez, J. A.; Truong, C. M.; Corneille, J. S.; Goodman, D. W. *J. Phys. Chem.* **1992**, *96*, 334.
(23) Truong, C. M.; Rodriguez, J. A.; Goodman, D. W. *J. Phys. Chem.* **1992**, *96*, 341.
(24) Rodriguez, J. A.; Truong, C. M.; Kuhn, W. K.; Goodman, D. W. *J. Chem. Phys.* **1992**, *96*, 740.
(25) Amberger, E. In *Gmelin Handbook of Inorganic Chemistry, Boron*, 8th ed.; Springer-Verlag: Berlin, 1981; Supplement Vol. 2.
(26) Amberger, E.; Dietz, W. In *Boron, Preparation, Properties and Applications*; Gaulé, G. K., Ed.; Plenum Press: New York, 1965; Vol. 2.
(27) Ugai, J. A.; Soloviev, N. E. In *Boron and Refractory Borides*, Matkovich, V. I., Ed.; Springer-Verlag: Berlin, 1977.
(28) Mavel, G.; Escard, J.; Costa, P.; Castaing, J. *Surf. Sci.* **1973**, *35*, 109–116.

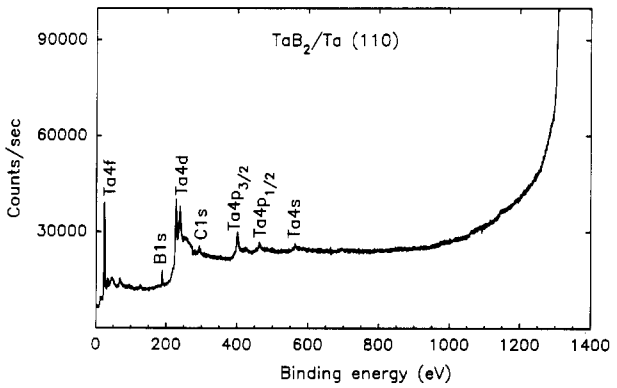

Figure 2. Full XPS spectrum of a typical TaB_2 layer before boron film growth.

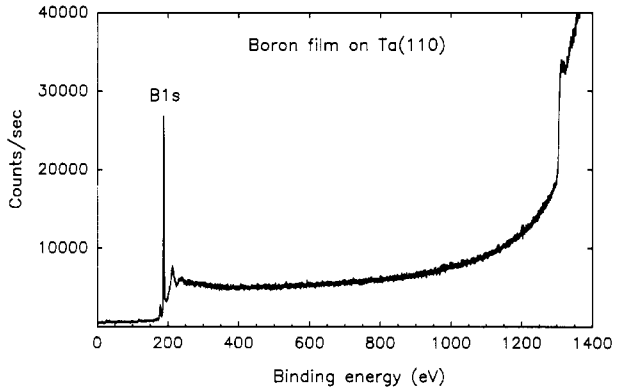

Figure 3. Full XPS spectrum of a CVD grown boron film.

mixture was directed toward the crystal through a doser with the chamber pressure at $\approx 5 \times 10^{-5}$ Torr. After more than 10 h, a boron film of sufficient thickness was obtained. Figure 3 shows a full XPS spectrum for a typical film. No features other than those of boron are observed. The spectrum is essentially the same as that of the clean β-rhombohedral boron (111) surface reported earlier where a full description of all of the features is given.[14] The absence of any Ta features in Figure 3 indicates that the thickness of the boron film must be at least 3 nm as this is the approximate escape depth of the Ta(4f) photoelectrons.

Part of our motivation for using a Ta single crystal as substrate was to determine if epitaxial TaB_2 could be grown. The lattice constants of the Ta(110) surface (a = 2.86 Å, b = 3.30 Å) are fairly close to those of TaB_2 which has a hexagonal structure with a = 3.08 Å, c = 3.27 Å. This suggests that epitaxial growth of TaB_2 with its c axis oriented along the Ta(110) normal might occur. However, only a blurry streaked LEED pattern of the TaB_2 layer was observed. Epitaxial growth of crystalline boron seems unlikely due to the large lattice mismatch between Ta(110) and the two most common crystalline phases of boron, β-rhombohedral (a = 10.94 Å for the (111) surface) or α-rhombohedral (a = 4.91 Å for the (111) surface)). Nevertheless, early reports show that crystalline boron can be grown by chemical vapor deposition on heated Ta wires.[25-27] The boron films that we prepared gave no discernible diffraction spots when examined with LEED. This is consistent with an amorphous boron film which would be expected from the relatively low growth temperatures.

For the oxygen reaction experiments, the chamber was backfilled with O_2 introduced through a leak valve. For the direct deposition of B_2O_2 or B_2O_3 on the boron film, sources similar to the B_2O_3 source described earlier were used.[14,17,18] A detailed description of the B_2O_2 source is given in the second of the present pair of papers. For the water experiments, D_2O was used so that a possible $DO^{11}BO$ desorption product would occur at m/e = 45 rather than at m/e = 44 for $HO^{11}BO$ which could be confused with background CO_2. The D_2O was introduced through a doser directed toward the sample. The use of a doser was necessary to prevent degradation of the vacuum. Because they were introduced in such different ways, it was not possible to quantitatively relate the O_2 and D_2O exposures.

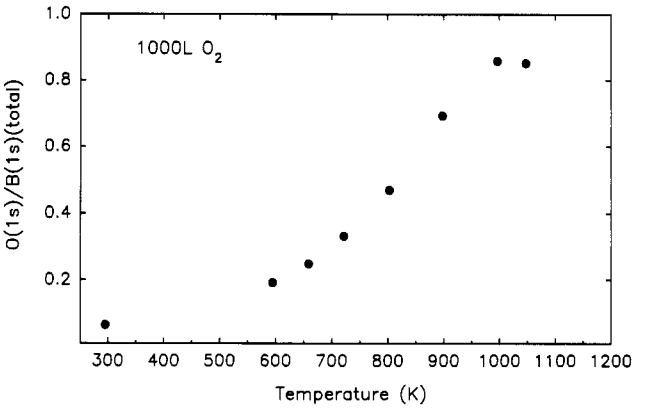

Figure 4. Plot of the O(1s)/B(1s) peak area ratio as a function of temperature for a 1000-langmuir O_2 exposure.

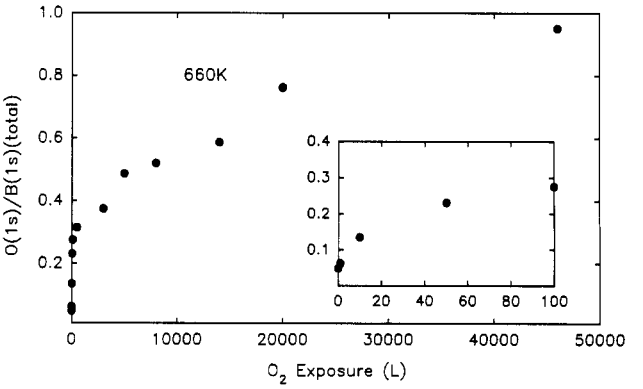

Figure 5. Plot of the O(1s)/B(1s) peak area ratio as a function of O_2 exposure at 660 K.

Results

XPS was used to monitor the uptake of oxygen by the boron films as a function of temperature. Figure 4 shows the O(1s)/B(1s) (total) peak area ratio at various temperatures following a 1000-langmuir O_2 exposure. The ratio increases with temperature and reaches a maximum between 1000 and 1100 K. Similar results were obtained on the single-crystal boron surface.[14] The B(1s) peak area is designated as "total" because it includes a chemically shifted peak due to oxidized boron, as discussed below, in addition to the one associated with elemental boron. Due to loss of boron through reaction with the Ta substrate and desorption of boron oxides, the data of Figure 4 were limited to temperatures $\leq$1100 K.

Figure 5 shows a plot of the O(1s)/B(1s) (total) ratio as a function of O_2 exposure at 660 K which shows that the oxygen uptake proceeds in two stages. For coverages corresponding to an O(1s)/B(1s) (total) ratio less than $\approx$0.5, the uptake is relatively rapid while for higher coverages the uptake occurs much more slowly. No saturation was observed even after a 5×10^4-langmuir O_2 exposure.

Although XPS shows that surface oxygen is removed from the boron surface by heating to temperatures above 1100 K, it cannot identify the oxygen containing species which desorbs. To answer this question, we obtained the temperature-programmed desorption (TPD) results shown in Figure 6 for two isotopes of B_2O_3 and B_2O_2 following a 4.6×10^4-langmuir O_2 exposure at 660 K. It is assumed that there is no desorption at this temperature. The TPD results demonstrate that B_2O_2 desorbs at 1100–1250 K and is the dominant desorption product with only a small amount of oxide desorbing as B_2O_3. During the course of

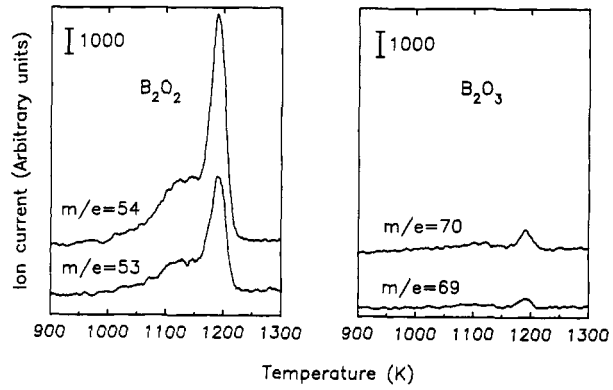

Figure 6. TPD results for four of the six possible B_2O_2 and B_2O_3 isotopes after a 4.6×10^4-langmuir O_2 exposure at 660 K with an initial O(1s)/B(1s) (total) peak area ratio of 0.938.

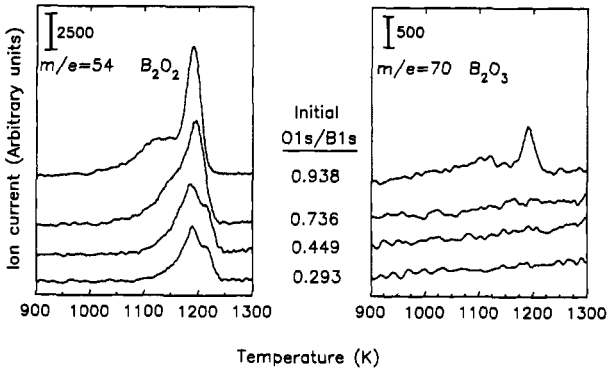

Figure 7. Variation of the $^{11}B_2O_2$ and $^{11}B_2O_3$ desorption peaks with initial O_2 exposure. The O_2 exposures were all at 660 K, and the amount of adsorbed oxygen is indicated by the O(1s)/B(1s) (total) peak area ratio.

these experiments several other mass channels were monitored including m/e = 10 (^{10}B), m/e = 11 (^{11}B), m/e = 26 (^{10}BO), m/e = 27 (^{11}BO), m/e = 38 ($^{11}B_2O$), and m/e = 43 ($^{11}BO_2$). Desorption of B_2O and BO_2 were not observed. The ^{10}B, ^{11}B, ^{10}BO, and ^{11}BO peaks occur at the same temperature as the B_2O_2 peak and occur in the same ratio to the B_2O_2 peak as in the mass spectrum of the B_2O_2 source as described in the following paper. The identification of the m/e = 10, 11, 26, and 27 peaks as due to B and BO is confirmed by the isotope ratio of ^{11}B:^{10}B = 4:1 which is characteristic of all boron-containing molecules. The mass spectrum of pure B_2O_3 consists primarily of the parent ion with only a small B_2O_2 fragment indicating that the results of Figure 6 are not due to B_2O_3 desorption.

The dependence of the oxide desorption on initial O_2 exposure provides some information on the desorption kinetics. Figure 7 shows the $^{11}B_2O_2$ (m/e = 54) and $^{11}B_2O_3$ (m/e = 70) TPD peaks as a function of increasing O_2 exposure. Due to the long period required for the boron film growth, only four sets of data were obtained. For the two lowest amounts of oxide we see a main peak at 1190 K with a shoulder at 1220 K which disappears at the higher oxide coverages. The asymmetry to lower temperatures in the third trace develops into a distinct new peak at 1125 K. The main peak remains constant at 1190 ± 4 K as the oxide coverage changes by over a factor of 3. Such behavior with coverage is characteristic of first-order desorption which indicates that the oxide is present at submonolayer coverages. A similar conclusion was reached in the single crystal study based on XPS data alone.[14]

Although we have identified B_2O_2 as the principal thermal desorption product, we have not yet established

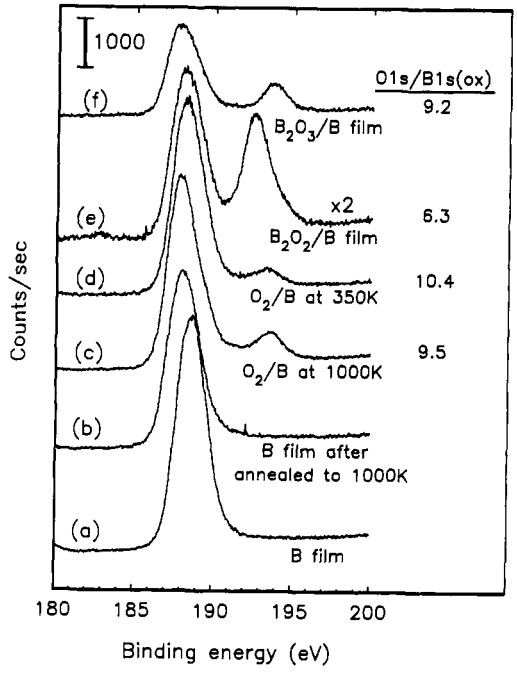

Figure 8. XPS spectra of the B(1s) region showing the position of the chemically shifted B(1s) peak of oxidized boron under the conditions indicated.

if B_2O_2 exists on the surface as a distinct molecular species prior to desorption or if it is simply produced at its desorption temperature as the product of some other surface chemical reaction. The question is whether the rate-limiting step for the appearance of B_2O_2(g) is desorption of adsorbed B_2O_2(ad) or formation of B_2O_2(ad) as the product of some other surface reaction. To address this issue, we have obtained XPS spectra of the boron surface on which B_2O_3 and B_2O_2 have been directly deposited from the gas phase for comparison with XPS spectra of the boron surface following reaction with O_2. Such a direct comparison is essential because a range of B(1s) binding energies for oxidized boron have been reported.[20,29,30] The results in the B(1s) region are given in Figure 8. These spectra were all taken at a constant analyzer pass energy of 20 eV which yields a resolution of 1.1 eV with Al Kα radiation.

In Figure 8 we see a B(1s) peak at 188.0 due to elemental boron and a chemically shifted B(1s) (ox) peak at higher binding energies due to oxidized boron. The oxidized boron is also characterized by the ratio of the O(1s) peak area to the B(1s) (ox) peak area. To obtain the peak areas, the B(1s) peaks were fit to a sum of two Gaussian functions after subtracting a linear baseline. The area of the higher binding energy Gaussian was taken as the B(1s) (ox) peak area. Figure 8f shows that directly depositing B_2O_3 onto the boron surface results in a B(1s) (ox) peak at 193.5 eV and a O(1s)/B(1s) (ox) peak area ratio of 9.2. Figure 8e shows that directly deposited B_2O_2 results in a B(1s) peak at 192.6 eV and a O(1s)/B(1s) (ox) peak area ratio of 6.3. In Figure 8d we see that exposure of the boron surface to O_2 at 350 K gives a B(1s) peak at 193.4 eV with a O(1s)/B(1s) (ox) peak area ratio of 10.4. Exposure to O_2 with the surface at 1000 K gives a larger B(1s) (ox) peak at 193.5 eV with a O(1s)/B(1s) (ox) peak area ratio of 9.5.

(29) Joyner, D. J.; Hercules, D. M. *J. Chem. Phys.* **1980**, *72*, 1095.
(30) Tavadze, F. N.; Nemoshkalenko, V. V.; Gabunia, D. L.; Senkevich, A. I.; Badzagua, T. S.; Tsiskarishvili, G. A.; Tsomaia, M. K. *J. Less-Common Met.* **1986**, *117*, 135.

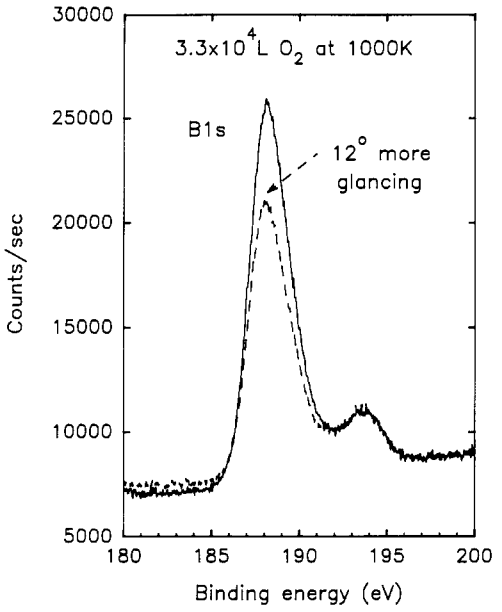

Figure 9. XPS B(1s) region at two different electron emission angles.

Comparison of the results of Figure 8d–f demonstrates that reaction of the boron with O_2 produces B_2O_3 and not B_2O_2 on the surface.

Also shown in Figure 8 is the effect on the B(1s) peak of annealing the boron film, which was grown at 650–700 K, to 1000 K. Annealing causes the B(1s) peak to shift from 188.6 eV in Figure 8a to 188.0 eV in Figure 8b. There is also a 25% decrease in intensity. The 0.6-eV shift may be due to slightly less charging in the annealed film of Figure 8b or to an effect due to an increase in the boron particle size associated with annealing.[31] The binding energy of 188.0 eV for the annealed boron film is close to that of single-crystal boron.[14]

Figure 9 shows the effect of changing the photoelectron detection angle on the relative height of the B(1s) peak of the oxidized and unoxidized boron following reaction with O_2. The two spectra have been offset to superimpose the oxidized B(1s) peak but have not been rescaled in any other way. The B(1s) (ox)/B(1s) peak area ratio clearly increases as the emission angle increases. This indicates that the oxide is concentrated at the surface and is not uniformly distributed over the photoelectron escape depth.

Figure 10 shows spectra of the B(1s) and O(1s) regions taken after annealing the sample to the indicated temperature following oxygen exposure at 600 K. All spectra were taken after the heating current was turned off and after the sample had cooled to 300–350 K. As shown in Figure 10b, the intensity of the O(1s) peak begins to decrease only after the sample has been heated to 1100 K. By 1250 K the intensity has dropped to zero. Comparison of Figure 10 with the TPD results of Figures 6 and 7 conclusively demonstrates that the surface oxide formed from the reaction of B with O_2 is completely removed mainly in the form of B_2O_2, accompanied by a small amount of B_2O_3 in the temperature range 1100–1250 K.

Annealing the oxidized surface leads to only modest changes in the B(1s) region. Since the boron films used in Figure 10a were not annealed prior to exposure to oxygen, the annealing causes a slight decrease in binding

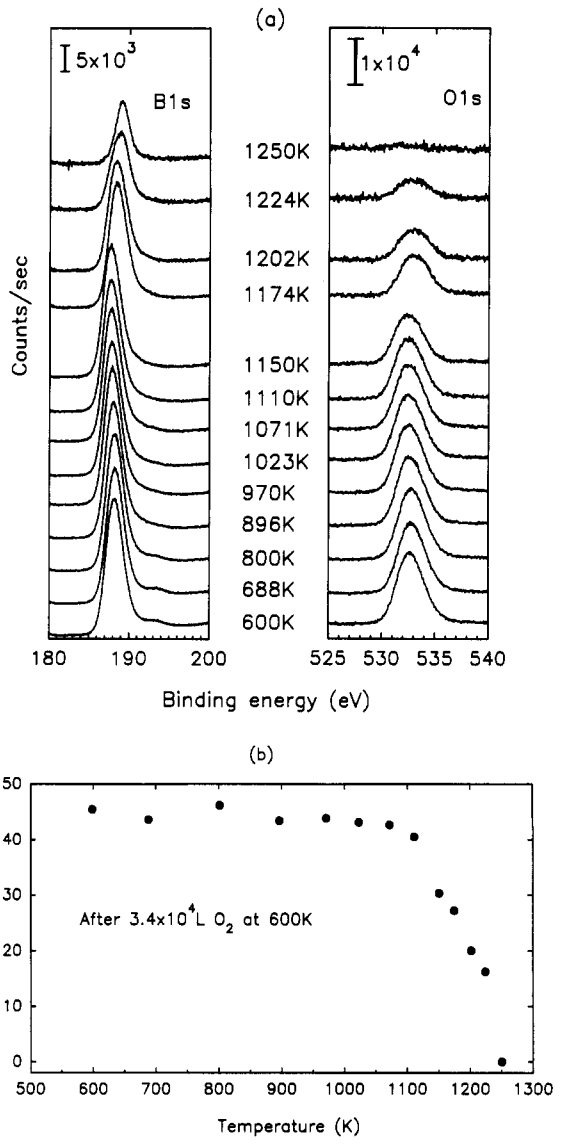

Figure 10. (a) XPS of the B(1s) and O(1s) regions as a function of the annealing temperature after an initial 3.4×10^4-langmuir O_2 exposure at 600 K. (b) Area of the O(1s) XPS peak as a function of temperature from the spectra of (a).

energy as noted in Figure 8. Thus the unoxidized B(1s) peak shifts from 188.3 eV from the 600 K spectrum to 188.0 eV for the 1023 K annealed spectrum. At 600 K the O_2 exposure used for this set of data yields an amount of oxide which gives rise to a barely perceptible B(1s) (ox) peak at 193.5 eV. This peak can no longer be detected after the 800 K anneal. At the four highest annealing temperatures we see that the B(1s) peak decreases in intensity and increases in binding energy to 189.0 eV. These changes are associated with incorporation of the boron into the Ta substrate to form TaB_2.

Virtually all of the results obtained with O_2 were also observed following D_2O exposures. The B(1s) region showed the development of a B_2O_3 peak at 193.4 eV following large D_2O exposures. A plot of the O(1s)/B(1s) peak area ratio as a function of D_2O exposure for a surface temperature of 750 K was similar to the plot in Figure 5 in that an initial oxygen uptake was followed by a much slower uptake. However, in the D_2O case the "plateau" occurred at a higher O(1s)/B(1s) ratio of $\approx$2.5. This may not be significant as the effective D_2O exposure achieved with the doser may have been much larger than the highest

(31) Rizzetti, A.; Xhie, J.; Sattler, K.; Yamamoto, D.; Pong, W. *J. Electron. Spectrosc. Relat. Phenom.* **1992**, *58*, 359.

O_2 exposures used. A plot of O(1s)/B(1s) as a function of temperature for a constant D_2O exposure was similar to the plot of Figure 4 although the highest temperature used, 800 K, was not high enough to observe a maximum in oxygen uptake. The TPD results following D_2O exposure were the same as with O_2 exposure. The dominant peak observed was that of B_2O_2 at a temperature of ≈1100 K. No DOBO desorption was observed. This was somewhat surprising as this compound is thought to be an important component in reaction mixtures containing B, O, and H.[8] Also, HOBO(g) was observed[32] to be the dominant species when H_2O(g) is in equilibrium with B_2O_3(l) in the range 1060–1450 K. We did not detect D_2 or any other compound containing D. This suggests that when D_2O reacts with the surface to produce B_2O_3, deuterium, presumably in the form of D_2, desorbs immediately. We would not detect this, as our TPD experiments are performed after the exposures are completed.

Discussion

The process of growing boron through chemical vapor deposition on tantalum substrates has a long history which has been thoroughly reviewed by Amberger.[25] By varying the substrate temperature and other growth conditions, different forms of elemental boron can be produced. At temperatures below ≈1200 K, glassy amorphous boron is produced; at intermediate temperatures of 1200–1500 K α-rhombohedral boron is formed; at temperatures above ≈1500 K the most stable allotrope, β-rhombohedral boron, is formed. The temperatures for growing these different forms are only approximate as the type of boron produced depends on other factors, such as growth rate; amounts and types of impurities; and pressure and composition of the precursor gases. In all cases, a thin nondiffusing layer of TaB_2 appears to form first with a thickness ranging from 0.01 to 0.1 mm depending on growth temperature.[25] Fairly large (0.25–2 mm) single crystals of either the α or β boron can apparently grow on the TaB_2 layer.[25-27] These methods generally employ thin Ta wires and flowing gases at pressures of 1–760 Torr. One of our goals was to determine if these flow-reactor CVD methods could be adopted for the in situ growth of boron under UHV conditions. This would then allow for the characterization of boron surface chemical properties with modern UHV surface science techniques. It was hoped that by adjusting the growth conditions, the different forms of elemental boron could be produced and their surface chemistry investigated.

In contrast to the methods described above, we found that although we could succeed in depositing a clean boron film on the Ta surface at low temperatures, annealing the boron film to temperatures above 1100 K resulted in the loss of surface boron as observed with XPS. Since the vapor pressure of boron is far too low at these temperature for any appreciable sublimation to occur, the loss of boron signal must be due to reaction of the boron with the Ta to form TaB_2. It would appear that what is described as a "thin" TaB_2 layer in the previous work would take a prohibitively long time to form under our growth conditions. A better approach for future work might be to grow the TaB_2 layer in a standard flow reactor external to the UHV chamber and then to transfer the sample to the UHV chamber for boron CVD.

(32) Meschi, D. J.; Chupka, W. A.; Berkowitz, J. *J. Chem. Phys.* **1960**, *33*, 530.

All previous work would indicate that the films grown at the low temperatures used here are of amorphous glassy boron. X-ray diffraction studies indicate that amorphous boron possesses short-range icosahedral ordering of the boron atoms and that it may represent structural features intermediate between that of α and β rhombohedral boron.[25] The techniques we have used, LEED and XPS, do not provide any information on the structure of the boron films other than their lack of long-range order. The shift of the B(1s) peak from 188.6 to 188.0 eV when a film deposited at 600–750 K is annealed to 1000 K may indicate some structural change, perhaps an increase in microcrystal particle size.[31] Regardless of the exact structure of the amorphous boron film, it provides a boron surface structurally distinct from the (111) surface of single-crystal β-rhombohedral boron. Comparison of the results obtained here with our previous results may thus provide some indication of the structure sensitivity of the reaction of boron with O_2.

The dependence of the O(1s)/B(1s) peak area ratio on O_2 exposure at a constant temperature plotted in Figure 5 and the dependence on temperature at constant exposure plotted in Figure 4 are qualitatively similar to the corresponding plots for the single-crystal boron surface.[14] However, a quantitative comparison shows that the amorphous film of the present study is somewhat more reactive. For example, in the present case we observe that the maximum oxygen uptake occurs at 1000–1050 K and in the previous case at 900–1100 K. At the maximum, the O(1s)/B(1s) ratio equals 0.86 for a 1000-langmuir exposure, while in the previous study the maximum ratio equaled 0.68 for a 5000-langmuir exposure. However, for exposures of 50 langmuirs we find a similar ratio of 0.25 for both surfaces. This suggests that while the net uptake of oxygen may be higher for high exposures on the amorphous film, the initial dissociative reaction probability for O_2 is approximately the same on the two surfaces.

The XPS spectrum of the oxidized surface provides some information on the nature of the oxide formed through the reaction with O_2. Through the direct deposition of B_2O_3 and B_2O_2 on the surface, we have established the identifying characteristics of these two boron oxides: an O(1s)/B(1s) peak area ratio of 6.3 ± 0.2 for B_2O_2 and 9.2 ± 0.2 for B_2O_3 and a B(1s) binding energy of 192.5 eV for B_2O_2 and 193.5 eV for B_2O_3. For the highest oxygen coverages we attained through O_2 exposures at both 350 and 1000 K, XPS results show that the oxide formed has the characteristics of B_2O_3 rather than of B_2O_2. Since we cannot detect the B(1s) (ox) peak at lower oxygen coverage we have no information on the chemical state of the initial oxide formed. In both the gas and condensed phases of B_2O_3 there are no B–B bonds, only B–O bonds. Gas-phase B_2O_2 and B_2O_2 trapped in noble-gas matrices have a O=B—B=O structure. No structural data on condensed B_2O_2 are available. The XPS results presented here and for the single-crystal boron study indicate that reaction with O_2 eventually produces an oxide in which boron is bonded only to oxygen as in B_2O_3. Obviously the oxide formed from the very first O_2 molecules which react with the surface must retain some B–B bonding and correspond to an oxide with a lower oxidation state than the +3 of B_2O_3. However, XPS provides insufficient sensitivity to detect the B(1s) peak of such an incipient oxide.

The use of temperature-programmed desorption has allowed us to show that the oxide is removed through heating primarily in the form of B_2O_2 with a smaller amount of B_2O_3. In our previous study on the single-crystal surface we were unable to identify the desorbing species because of experimental difficulties associated with mounting the sample. Given the other similarities between that study and the present one, we assume that the oxygen was also removed as B_2O_2 from the single-crystal surface. The fact that essentially no oxygen uptake was observed at 1273 K in the earlier study is consistent with the B_2O_2 desorption peak at 1190 K observed here. The desorption of B_2O_2 from surfaces containing boron has been observed in several other cases.[33-37] In an earlier paper we reported that B_2O_3 directly deposited on the single-crystal boron surface will react with the substrate to produce B_2O_2 and that a smaller B_2O_3 peak occurs at the same temperature.[17] The TPD results are thus completely consistent with the formation of a small amount of B_2O_3 on the surface as detected by XPS. The reaction of B_2O_3 with boron to produce B_2O_2 is a well-known reaction and has been used to prepare B_2O_2 for spectroscopic characterization.[38-40] The properties and reactions of both B_2O_3 and B_2O_2 directly deposited on the boron films grown as described here are fully described in the following paper.

(33) Ozcomert, J. S. Ph.D. Dissertation, University of Illinois at Chicago, 1992.
(34) Ozcomert, J. S.; Trenary, M., to be published.
(35) Davis, P. R.; Chambers, S. A. *Appl. Surf. Sci.* **1981**, *8*, 197.
(36) Inghram, M. G.; Porter, R. F.; Chupka, W. A. *J. Chem. Phys.* **1956**, *25*, 498.
(37) Kiss, J.; Révész, K.; Solymosi, F. *Appl. Surf. Sci.* **1989**, *37*, 95.
(38) Weltner, W., Jr.; Warn, J. R. W. *J. Chem. Phys.* **1962**, *37*, 292.
(39) Sommer, A.; White, D.; Linevsky, M. J.; Mann, D. E. *J. Chem. Phys.* **1963**, *38*, 87.
(40) Rušcić, B. M.; Curtiss, L. A.; Berkowitz, J. *J. Chem. Phys.* **1984**, *80*, 3962.

Conclusions

Diborane can be used to grow clean boron films of arbitrary thickness on Ta(110) at temperatures below 1100 K. At higher temperatures the boron reacts with the substrate to form TaB_2. This reaction prevents transforming the initially deposited amorphous film into crystalline boron by annealing to higher temperatures.

The boron films show a temperature-dependent reactivity toward O_2 which changes by a factor of 8 between 300 and 1000–1100 K where the reactivity reaches a maximum. Even at 1000–1100 K the reactivity is low with exposures of 1×10^3 langmuirs producing less than a monolayer of oxide.

Thermal desorption results show that the surface oxide is removed predominantly through the desorption of B_2O_2 with a smaller amount desorbing as B_2O_3 in the temperature range 1100–1250 K.

At the highest oxide coverages achieved through reaction with O_2, XPS results show that the oxide is B_2O_3 rather than B_2O_2. This implies that at temperatures above 1100 K the surface B_2O_3 reacts with the boron substrate to produce $B_2O_2(g)$. At this temperature, some unreacted B_2O_3 also desorbs.

The reaction with water also produces surface B_2O_3 which then displays the same behavior as surface B_2O_3 produced from the reaction with O_2.

Acknowledgment. This work was supported by a grant (AFOSR-92-J-0179) from the Air Force Office of Scientific Research.